Zinc stable isotope analysis reveals Zn dyshomeostasis in benign tumours, breast cancer, and adjacent histologically normal tissue

Kaj V. Sullivan,*[a,b] Rebekah E. T. Moore,[b] Miles S. Capper,[b] Kathrin Schilling,[c] Kate Goddard,[d] Charlotte Ion,[d] Daniel Layton-Matthews,[a] Matthew I. Leybourne,[a,e] Barry Coles,[b] Katharina Kreissig,[b] Olga Antsygina,[f,g] R. Charles Coombes,[d] Fiona Larner,[h,i,j] Mark Rehkämper[b]

*Corresponding author E-mail: kajvsullivan@gmail.com; Tel: +1 (613)-985-4166; Mailing address: 67 Robinhood Drive, L9H 4G2, Dundas ON, Canada

[a] Department of Geological Sciences and Geological Engineering, Queen's University, 36 Union Street, Kingston, K7L 2N8, Canada.

[b] Department of Earth Science & Engineering, Imperial College London, Exhibition Road, London, SW7 2AZ, UK

[c] Lamont-Doherty Earth Observatory, Columbia University, Palisades, NY, 10964, US

[d] Dept of Surgery and Cancer, Imperial College, ICTEM, Hammersmith Hospital, Du Cane Rd, London W12 ONS, UK

[e] Arthur B. McDonald Canadian Astroparticle Physics Research Institute, Department of Physics, Engineering Physics & Astronomy, Queen's University, 64 Bader Lane, Kingston, K7L 3N6, Canada

[f] Healthy Active Living and Obesity Research Group, Children's Hospital of Eastern Ontario Research Institute, Ottawa, ON, K1H 8L1, Canada

[g] Department of Health Sciences, Carleton University, Ottawa, ON, K1S 5B6, Canada

[h] Department of Earth Sciences, University of Oxford, South Parks Road, Oxford, OX1 3AN, UK

[i] St Catherine's College, Manor Road, Oxford, OX1 3UJ, UK

[j] Science & Technology Facilities Council, Rutherford Appleton Laboratory, Harwell Campus, Didcot, OX11 0DE, UK

Running head (50 characters of less): Breast cancer Zn stable isotope dyshomeostasis

Abstract

The disruption of Zn homeostasis has been linked with breast cancer development and progression. To enhance our understanding of changes in Zn homeostasis both inside and around the tumour microenvironment, Zn concentrations and isotopic compositions (δ^{66}Zn) were determined in benign (BT) and malignant (MT) tumours, healthy tissue from reduction mammoplasty (HT), and histologically normal tissue adjacent to benign (NAT(BT)) and malignant tumours (NAT(MT)). Mean Zn concentrations in NAT(BT) are 5.5 μg g^{-1} greater than in NAT(MT) (p = 0.00056) and 5.1 μg g^{-1} greater than in HT (p = 0.0026). Zinc concentrations in MT are 12.9 μg g^{-1} greater than in HT (p = 0.00012) and 13.3 μg g^{-1} greater than in NAT(MT) (p < 0.0001), whereas δ^{66}Zn is 0.17‰ lower in MT than HT (p = 0.017). Benign tumour Zn concentrations are also elevated compared to HT (p = 0.00013), but are not significantly elevated compared to NAT(BT) (p = 0.32). The δ^{66}Zn of BT is 0.15‰ lower than in NAT(BT) (p = 0.045). The similar light δ^{66}Zn of BT and MT compared to HT and NAT may be related to the isotopic compensation of increased metallothionein (^{64}Zn-rich) expression by activated matrix metalloproteinase (^{66}Zn-rich) in MT, and indicates a resultant ^{66}Zn-rich reservoir may exist in patients with breast tumours.

Zinc isotopic compositions thus show promise as a potential diagnostic tool for the detection of breast tumours. The revealed differences of Zn accumulation in healthy and tumour-adjacent tissues requires additional investigation.

Introduction

Zinc (Zn), with its five stable isotopes (^{64}Zn, ^{66}Zn, ^{67}Zn, ^{68}Zn, and ^{70}Zn), typically occurs in the divalent (Zn^{2+}) form, and is the second most abundant transition metal in organisms after iron (Fe) [1]. This reflects that Zn is a component of approximately 3000 human proteins [2] and has many roles in the body, including contributing to normal growth and development, immunity, cellular homeostasis, cell survival, and biochemical functions [1,3,4]. Zinc also catalyses reactions, stabilizes protein structures, and is a cofactor or component of more than 300 metalloenzymes [1,5]. The Zn content of the human body ranges from 1.5 to 3 g and the total cellular Zn concentrations are in the several hundred micromolar range [6]. With an absolute daily Zn requirement of 2 to 3 mg, the recommended daily intake of an adult is approximately 10 mg, resulting in a turnover time in the body of 150 to 300 days [7–9].

In the late 1990s, the development of multi-collector inductively coupled plasma mass spectrometry (MC-ICP-MS) and ion exchange chromatography procedures, which can efficiently purify metals and metalloids from even complex sample matrices prior to isotopic analysis, enabled rapid measurements (compared to thermal ionisation mass spectrometry) that are able to routinely resolve subtle changes in the isotope amount ratios of Zn and other metals such as copper (Cu) and Fe in a diverse range of natural samples [10,11]. This advance opened a new

64 research frontier for planetary, earth, and environmental scientists and also enabled the first
65 investigations of metal stable isotope distribution in the human body, and the processes that
66 govern their allocation [11]. Since then, investigators have sought to establish a stable isotope
67 reference range for Cu, Fe, Zn, and other elements in the blood compartments, cerebrospinal
68 fluid, and urine of healthy subjects so as to understand changes observed in those suffering from
69 diseases where metal dyshomeostasis is fundamental to disease pathogenesis [12–33]. This
70 includes breast cancer, where the dysregulation of Zn homeostasis is implicated in carcinogenesis
71 [34,35].

72 The histidine-rich Zn-regulated transporter (ZRT), Fe-regulated transporter (IRT)-like
73 protein (ZIP) family, and Zn transporter proteins (ZnT) facilitate Zn homeostasis in normal cells
74 [36]. Zinc homeostasis breaks down in cancerous cells due to the increased expression of Zn
75 importers (ZIP5, ZIP6 (LIV-1), ZIP7, ZIP8, and ZIP10), which produce an influx of Zn into cancer
76 cells [34,35]. The anti-oxidant protein metallothionein (responsible for buffering cytosolic Zn) is
77 also crucial to Zn homeostasis in normal cells, despite binding only a small portion of total cellular
78 Zn (in the nano- to picomolar range) [6]. In malignant breast cancer cells, ZnT2 and
79 metallothionein are also overexpressed, providing protection from Zn hyperaccumulation and
80 preventing apoptosis by either removing Zn from the cell or redistributing it among cellular
81 compartments [37,38].

82 It is not known whether the malfunction of Zn-binding proteins causes or results from
83 tumourigenesis [39]. The trend towards ZIP upregulation in most cancers may indicate increased
84 cellular Zn uptake requirements to meet the demands of increased rate of proliferation and
85 metabolism [39]. This excess Zn may also be used to induce Zn-dependent processes. Such

processes include metastasis, angiogenesis, and the production of matrix metalloproteinases (MMPs) - a family of Zn-dependent endopeptidases that are capable of digesting extracellular matrix (ECM) and basement membrane [40,41]. The ECM is a framework of proteins and proteoglycans secreted by stromal fibroblasts that gives structural support to cells and is important to cell adhesion, differentiation, proliferation, and migration [41]. Cancer cell migration, invasion, metastasis, and angiogenesis are all dependent on the surrounding tumour microenvironment [42]. MMPs are critical molecules in these processes because they degrade various cell adhesion molecules in ECM, thereby giving cancer cells access to new territories [42].

Recent pilot work indicates that malignant breast tumours may preferentially accumulate isotopically light ^{64}Zn compared to adjacent histologically normal tissue [43]. This was hypothesized to be caused by S-rich metallothionein dominating the isotopic selectivity of breast cancer cells, rather than histidine-rich ZIPs and ZnTs. Unlike Cu, for which oxidation state plays a significant role in isotope fractionation, fractionation of Zn isotopes in compounds is predominantly influenced by coordination number and ligand chemistry. Higher mass isotopes tend to concentrate in compounds that provide stronger chemical bonds with the lower energy levels, and to a first order, the strength of the bond is expected to increase with ionization energy or electronegativity from sulfur (S) through nitrogen (N) to oxygen [17,25]. For example, Zn binding with cysteine (Zn-S bonds) in metallothionein is expected to be more concentrated in the light isotope, ^{64}Zn, than in bonds with histidine (Zn-N bonds) [17,44]. Furthermore, recent studies demonstrate that Zn isotopes are significantly fractionated in conditions such as pancreatic ductal carcinoma (PDAC) [29] and hematological malignancy [20], which leads to isotopic changes

107 in Zn reservoirs including urine and blood, respectively. These results demonstrate that Zn
108 isotopes are potentially useful diagnostic and prognostic markers for various medical conditions.
109 This study provides new insights into the disruption of Zn homeostasis during malignant
110 breast tumour growth through elemental and isotopic analysis of Zn in healthy breast tissue
111 taken during reduction mammoplasty (HT), histologically normal tissue adjacent to malignant
112 tumours, (NAT(MT)), and malignant breast tumours (MT). Additionally, for the first time, Zn
113 isotope compositions of benign breast tumours (BT) and histologically normal tissue adjacent to
114 benign tumours (NAT(BT)) are analysed to determine whether the enrichment in light ^{64}Zn is
115 specific to malignant breast tumours or also observed in the benign condition. Where possible,
116 NAT(BT)-BT and NAT(MT)-MT tissue sample pairs were therefore taken from the same patient.
117 High levels of Zn in the breast tissue of women with benign breast disease may be associated
118 with a modest risk of developing malignancy [45] and this research will help evaluate whether Zn
119 stable isotopes have the potential to serve as diagnostic markers of breast cancer.
120 Notably, this is the first instance of a comparison of Zn concentrations and isotopic
121 compositions in the three "healthy" tissue types, HT, NAT(BT), and NAT(MT), as well as both BT
122 and MT. Histologically normal tissue adjacent to tumours commonly serves as a healthy control
123 sample for cancer studies, but evidence suggests that NAT presents a unique intermediate, pre-
124 neoplastic state between healthy and tumour tissue [46,47], composed of morphologically
125 normal but molecularly altered cells [48]. The latter findings call into question the assumption
126 that histological normalcy implies biological normalcy [46]. The results of this study thus enhance
127 our understanding of changes in Zn homeostasis both inside and around the tumour
128 microenvironment.

Methodology

Sample collection

This study received approval from the Tissue Management Committee of the Imperial College National Institute of Healthcare (NHS) Tissue Bank (Application Number: R15001-6A). Sample collection took place between May 2015 and November 2016 at Charing Cross Hospital, Imperial College London, NHS Trust, London, UK. Benign and malignant breast tumours (BT and MT), along with histologically normal tissue adjacent to tumours (NAT) were taken from patients. Healthy breast tissue was taken from volunteers undergoing reduction mammoplasty. Where possible, pairs of tumour and NAT samples were obtained from the same patient. Tissue samples were taken during surgery using pre-cleaned ceramic knives and stored at -18°C in separate sterile VWR® Metal-Free polypropylene centrifuge tubes, which were cleaned in 2 mol L^{-1} HNO_3 for two days before being rinsed with 18.2 MΩ cm H_2O and left to dry. Histologically normal tissue adjacent to tumours was dissected beyond observed aberrations.

Sample preparation

Sample preparation was performed under ISO Class 4 metal-free laminar flow hoods either in the MAGIC Clean Room Laboratory at Imperial College London or in the Clean Laboratory Suite at the University of Oxford. Distilled acids diluted with ≥18.2 MΩ cm H_2O (Millipore) were used throughout sample preparation. Between 0.02 and 0.89 g of wet sample was mixed with

149 5.2 ml of 15 mol L^{-1} HNO_3 and 2.8 ml of 30% H_2O_2 in acid-cleaned 100 ml PFA vessels and allowed
150 to stand overnight before being microwave digested using either an Ethos EZ oven fitted with an
151 SK-10 High Pressure Rotor or a MARS 5 Digestion Microwave System, for 90 minutes, ramping up
152 to a temperature of 210°C at a pressure of 1.72 x 10^6 Pa. Separation of Zn from matrix elements
153 was achieved by anion exchange column chromatography using Bio-Rad AG® MP-1M (100-200
154 mesh) resin in hydrochloric acid media [49].
155
156 **Concentration measurements and isotopic analysis**
157 An initial determination of Zn concentrations by isotope dilution was carried out for each
158 sample to ensure that an appropriate sample aliquot was digested for isotopic analysis. The
159 sample solutions were mixed in optimal proportion (molar ratio of spike-derived to natural Zn of
160 S/N ≈ 1) with a ^{64}Zn-^{67}Zn double spike ($^{64}Zn/^{67}Zn$ ≈ 2.5) to enable the correction of any isotope
161 fractionation incurred during chromatographic separation and isotopic analysis. Following the
162 addition of Zn double spike solution to the digested sample aliquots that were re-dissolved in 2
163 mol L^{-1} HCl, the mixtures were refluxed on a hot plate at 130°C for at least 12 hours to allow the
164 samples to fully equilibrate with the double spike [49,50].
165 The coupled Zn isotope and concentration measurements with the double spike
166 technique followed previously described techniques [49,51]. Measurements were performed on
167 a Nu Plasma HR MC-ICP-MS (Nu Instruments Ltd., Wrexham, UK) at low mass resolution with
168 either an Aridus II (Teledyne CETAC Technologies, Omaha, US) or a DSN-100 desolvation system
169 (Nu Instruments Ltd.) for sample introduction fitted with glass nebulizers that had a typical

uptake rate of approximately 100 to 120 μl min^{-1}. With an instrumental sensitivity of about 120 V ppm^{-1} for the Faraday cup detectors fitted with 10^{11} Ω resistors, the isotope analyses were performed at Zn concentrations of 50 to 100 ng g^{-1}. The sample solutions were run interspersed between and relative to analyses of the isotopic reference material, IRMM-3702 Zn (also mixed with the double spike at S/N ≈ 1), to monitor and correct for within- and between-session changes in instrumental mass bias [49,51].

As natural variations in the ratio (R), $^{66}Zn/^{64}Zn$, are small, isotopic data are reported in $\delta^{66}Zn$ notation, which denotes the parts per thousand (‰) change in the $^{66}Zn/^{64}Zn$ value of a sample relative to a standard (Std; Equation 1).

$$\delta^{66}Zn_{Std}\ (‰) = \left(\frac{R_{Sample}}{R_{Standard}} - 1\right) 1{,}000 \qquad (1)$$

The $\delta^{66}Zn$ values, originally determined relative to IRMM-3702 Zn ($\delta^{66}Zn_{IRMM}$), were recalculated so that all results are given relative to the JMC-Lyon Zn isotope reference material ($\delta^{66}Zn_{JMC\text{-}Lyon}$) using Equation 2 [52].

$$\delta^{66}Zn_{JMC-Lyon} = \left[\left(\frac{\delta^{66}Zn_{IRMM}}{1{,}000} + 1\right)\left(\frac{\Delta^{66}Zn_{IRMM-JMC}}{1{,}000} + 1\right) - 1\right] 1{,}000 \qquad (2)$$

A value of 0.30‰ was used for the $\delta^{66}Zn$ offset between IRMM-3702 and JMC-Lyon Zn ($\Delta^{66}Zn_{IRMM\ -\ JMC\text{-}Lyon}$), based on results from the interlaboratory calibration of the new Zn isotope reference material, AA-ETH Zn ($\Delta^{66}Zn_{AA-JMC}$ = –0.28‰ and $\Delta^{66}Zn_{AA-IRMM}$ = 0.02‰) [52].

Statistical analysis

Statistical analyses were conducted using SAS Studio 3.8 software (SAS Institute). Because the assumption of normality was not fulfilled (assessed using Shapiro-Wilk's test), the non-parametric Kruskal-Wallis test was used to compare Zn concentrations and δ^{66}Zn between tissues types. An analysis of within-group variations was performed using the Wilcoxon signed-rank test to compare Zn concentrations and δ^{66}Zn in patients that provided both NAT and tumour samples, allowing for the control of possible variability in Zn concentrations and δ^{66}Zn associated with age, diet and medication uptake. The relationship between Zn concentrations and δ^{66}Zn for benign and malignant breast tumours was assessed using the Spearman rank correlation coefficient (ρ). P-values of less than 0.05 were considered statistically significant. No correction was made for multiple comparisons. The δ^{66}Zn could not be obtained for some samples due to limited availability of material, resulting in an insufficient amount of Zn for isotopic analysis. Additionally, some samples were damaged during transport between facilities for isotopic analysis. In detail, δ^{66}Zn data is missing for 18% of HT, 13% of NAT(BT), 5% of NAT(MT), 6% of BT, and 10% of MT samples and missing data were excluded from statistical analyses.

Results

Quality control

Zinc blank contributions were monitored and remained below 1.5 ng, which is equivalent to less than 0.8% of total sample Zn. Assuming a 'normal' terrestrial δ^{66}Zn of 0.25‰ for the blank, the δ^{66}Zn value of a sample with –0.66‰ (the lowest measured in this study) will be biased by less than 0.01‰ by the contamination, which is negligible given the overall uncertainty of the results [50,53,54].

Following the collection of raw data, the double spike data reduction was performed offline using an iterative procedure developed by Siebert *et al*. that corrects for instrumental mass bias and ion exchange chromatography-induced mass fractionation [55]. Spectral interferences from isobars ($^{64}Ni^{+}$) and doubly-charged ions (Ba^{2+}) were monitored at masses 60 ($^{60}Ni^{+}$) and 67.5 ($^{135}Ba^{2+}$), respectively, and the corrections were propagated through the iterative data reduction to ensure they are adjusted for instrumental mass bias [50]. The applied corrections were consistently very small. In detail, contributions to the ion beam at mass 64 from $^{64}Ni^{+}$ were ≤ 15 ppm for samples and ≤ 2 ppm for bracketing runs of the IRMM-3702 Zn standard. Furthermore, interferences from doubly-charged Ba were < 1ppm at $^{132}Ba^{2+}/^{66}Zn$, ≤ 5 ppm at $^{134}Ba^{2+}/^{67}Zn$, and ≤ 25 ppm at $^{136}Ba^{2+}/^{68}Zn$ for samples and < 1ppm at $^{132}Ba^{2+}/^{66}Zn$, ≤ 5 ppm at $^{134}Ba^{2+}/^{67}Zn$, at ≤ 20 ppm for $^{136}Ba^{2+}/^{68}Zn$ for IRMM-3702 Zn runs. At these levels, even unreasonably large errors in the interfering element corrections (of ±10%) have negligible effects (of < 0.01‰) on the final δ^{66}Zn data. Analytical artefacts are further de-magnified by the comparatively similar interference levels of samples and the bracketing IRMM-3702 Zn runs, relative to which δ^{66}Zn sample values are determined. Consequently, the 2SD precisions that are reported for most samples refer to the 2SD reproducibility that was obtained for bracketing

231 standard measurements (IRMM-3702 Zn), which were performed alongside samples in a given
232 measurement session. These precisions varied from ± 0.03 to ± 0.12‰.

233 With blank and interference contributions to uncertainty being negligible, mass
234 spectrometric uncertainty is primarily responsible for the total δ^{66}Zn uncertainty, and this is
235 predominantly limited by the instability of the instrumental mass bias [50]. To a first order, the
236 mass spectrometric uncertainty can hence be characterized by the reproducibility of δ^{66}Zn values
237 determined for replicate analyses of a London Zn – Zn double spike mixture [50]. During this
238 study, this was ± 0.08‰ (2SD) for column-processed mixtures and ± 0.04‰ (2SD) for mixtures
239 that did not undergo column chemistry.

240 The method reproducibility was monitored by repeat analyses of sample solutions, and
241 by measuring both unprocessed and column-processed aliquots of the in-house London Zn
242 solution throughout measurement sessions, which yielded mean δ^{66}Zn of 0.12 ± 0.04‰ (2SD, *n*
243 = 3) and 0.13 ± 0.08‰ (2SD, *n* = 5), respectively. The London Zn δ^{66}Zn reported here, as well as
244 the repeatability and intermediate precision, are in accord with previously published results
245 [43,49,50,52,56,57]. However, repeated analyses of pure Zn standard solutions do not account
246 for mass spectrometric uncertainties that can arise for samples as a consequence of non-spectral
247 matrix effects. To account for this, two relevant matrix-matched biological reference materials,
248 ERM-BB184, bovine muscle, and ERM-BB186, pig kidney, were analyzed throughout the study
249 period and column-processed alongside with tissue samples. Analyses of these samples yielded
250 mean δ^{66}Zn of 0.03 ± 0.12‰ (2SD, *n* = 10) and -0.38 ± 0.14‰ (2SD, *n* = 9), respectively, relative
251 to JMC-Lyon Zn. This is in excellent agreement with previously reported results [32,49].

252 Where sufficient material was available, sample homogeneity was assessed by splitting
253 samples into two aliquots and analyzing separately. Although homogeneity could only be
254 assessed for three samples, variations in δ^{66}Zn are within analytical precision (< 0.12‰, 2SD) for
255 both 'normal' tissues and the benign tumour, whereas variations in Zn concentrations for the
256 benign tumour are greater than in 'normal' tissues (Supplementary Information Table S1).

257

258 **Zinc concentrations and δ^{66}Zn in unpaired samples**

259 Determined in this study were Zn concentrations (Table 1, Supplementary Information
260 Table S2) for 69 breast tissue samples (10 HT, 8 NAT(BT), 16 NAT(MT), 17 BT, 17 MT) and δ^{66}Zn
261 for 62 tissue samples (8 HT, 7 NAT(BT), 15 NAT(MT), 17 BT, 15 MT) (Table 2, Supplementary
262 Information Table S2). All benign tumours are fibroadenomas except for one tubular adenoma
263 and one phyllodes tumour. Invasive ductal carcinoma (IDC) was identified in all breast cancer
264 patients for whom breast cancer type was available (Supplementary Information, Table S2). In
265 addition to the presence of IDC, ductal carcinoma *in-situ* (DCIS) was identified in nine patients
266 and lobular carcinoma *in-situ* in one (Supplementary Information, Table S2). Invasive ductal
267 carcinoma is the most common type of breast cancer and accounts for 50 to 70% of breast
268 cancers in previously published series [58,59]. Included in all subsequent descriptions and
269 interpretations are results from Larner *et al*., which consists of data for one HT, three NAT(MT),
270 and five MT [43].

271 When tissue taken during reduction mammoplasty and both types of NAT are considered
272 together as nominally 'normal' tissue, Zn concentrations range from 0.4 to 14.0 $\mu g\ g^{-1}$ with a

mean of 3.6 ± 3.3 μg g^{-1} (SD), and δ^{66}Zn varies from -0.61 to 0.23‰ with a mean of -0.22 ± 0.19‰ (SD). Considered separately, Zn concentrations in HT and NAT(MT) are similar, with HT ranging from 0.6 to 6.5 μg g^{-1} with a mean of 2.3 ± 1.7 μg g^{-1} (SD), and NAT(MT) ranging from 0.4 to 7.4 μg g^{-1} with a mean of 1.9 ± 1.6 μg g^{-1} (SD) (Table 1). In contrast, Zn concentrations in NAT(BT) are significantly elevated compared to HT and NAT(MT) (p = 0.0026 and p = 0.00056, respectively) and range from 2.4 to 14.0 μg g^{-1} with a mean of 7.4 ± 4.4 μg g^{-1} (SD) (Table 1). Despite the elevated NAT(BT) Zn concentrations, there is little variation in δ^{66}Zn amongst the 'normal' tissues, with HT ranging from -0.37 to -0.01‰ with a mean of -0.20 ± 0.13‰ (SD), NAT(BT) ranging from -0.33 to 0.00‰ with a mean of -0.17 ± 0.15‰ (SD), and NAT(MT) ranging from -0.61 to 0.23‰ with a mean of -0.25 ± 0.23‰ (SD) (Table 2).

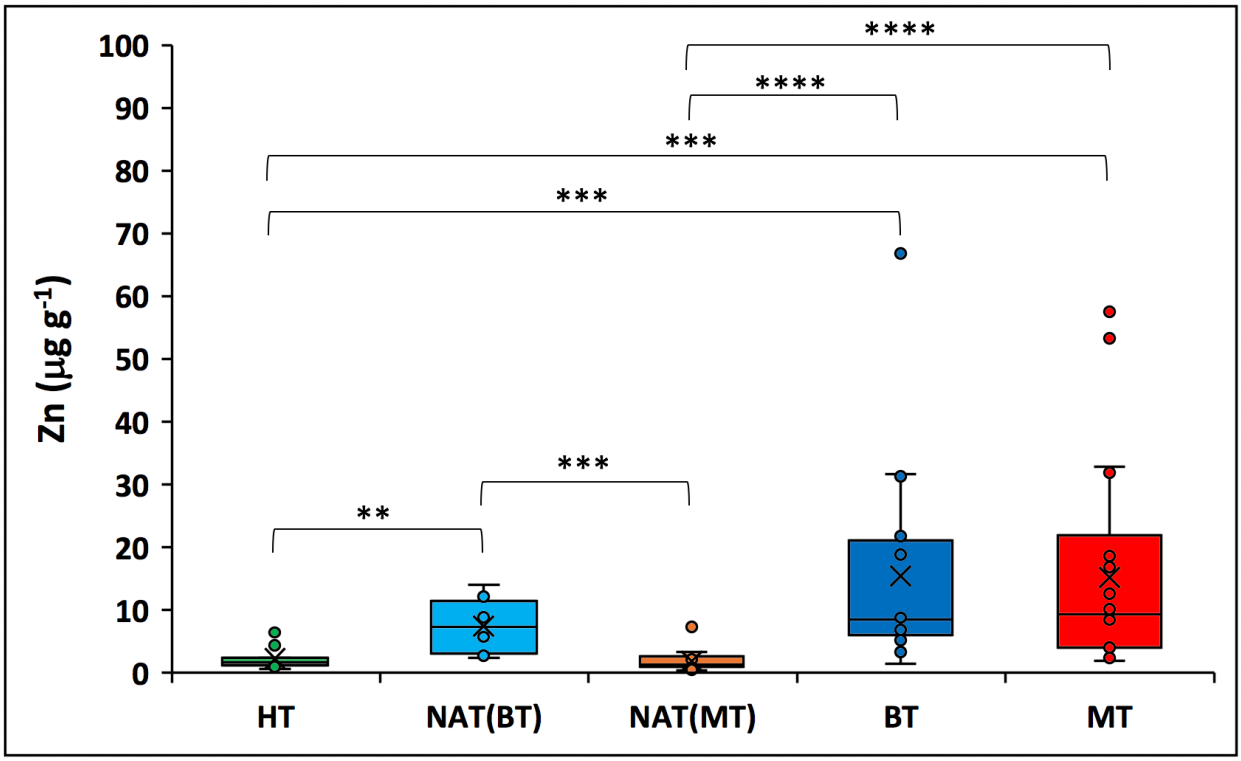

Figure 1 Zinc concentrations in healthy breast tissue taken during breast reduction surgery (HT); histologically normal tissue adjacent to benign tumour, NAT(BT); histologically normal tissue

adjacent to malignant tumour, NAT(MT); benign tumour, BT; and malignant tumour, MT. The box represents the 25th-75th percentiles (with the median as a horizontal line) and the whiskers represent the range. Outliers are denoted outside of the range if they exceed a distance of 1.5 times the interquartile range below the 1st quartile or above the 3rd quartile. The thresholds for significance were defined as $p < 0.05$ (*), $p < 0.01$ (**), $p < 0.001$ (***), and $p < 0.0001$ (****). All other relationships displayed no statistical significance ($p \geq 0.05$). Data from HT, NAT(MT), and MT measured by Larner *et al*. are included [43].

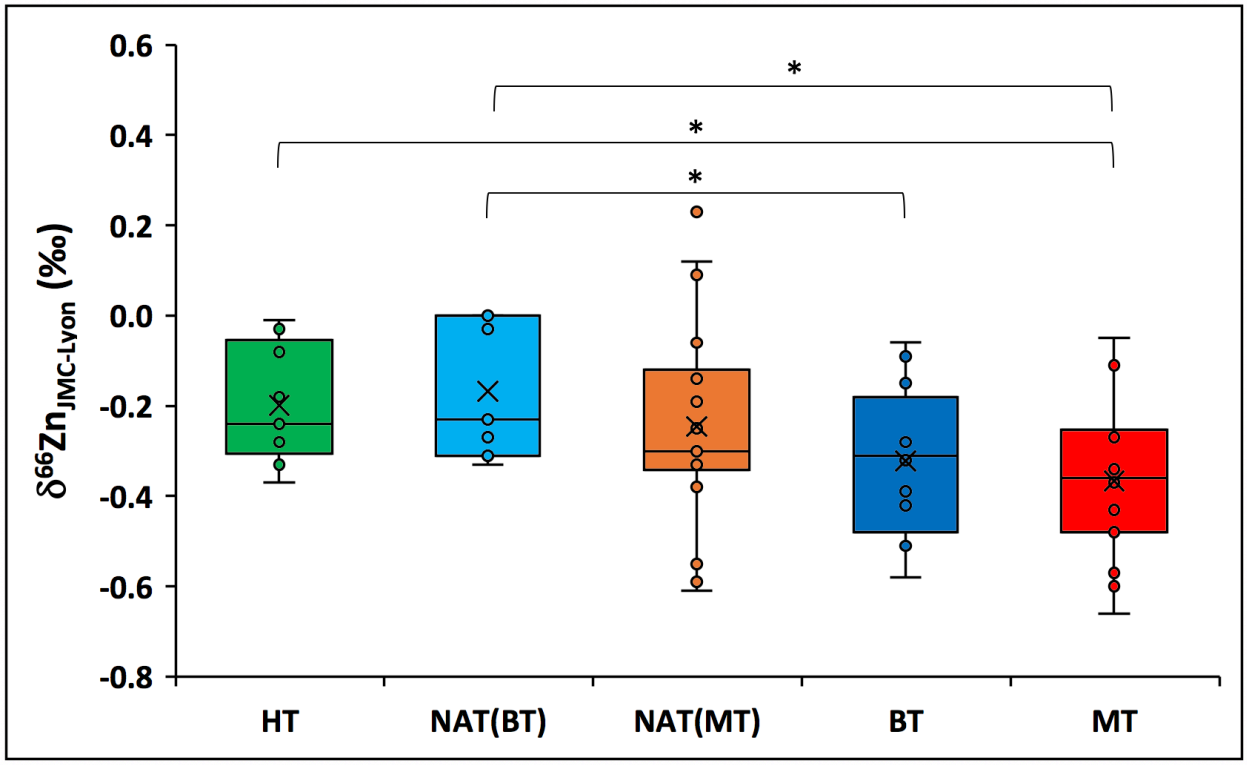

Figure 2 δ^{66}Zn variations in healthy breast tissue taken during reduction mammoplasty (HT); histologically normal tissue adjacent to benign tumour, NAT(BT); histologically normal tissue adjacent to malignant tumour, NAT(MT); benign tumour, BT; and malignant tumour, MT. The box represents the 25th-75th percentiles (with the median as a horizontal line, median as a cross) and the whiskers represent the range. Outliers are denoted outside of the range if they exceed a distance of 1.5 times the interquartile range below the 1st quartile or above the 3rd quartile. The threshold for significance was defined as $p < 0.05$ for significant results (*). All other relationships displayed no statistical significance ($p \geq 0.05$). Data from HT, NAT(MT), and MT measured by Larner *et al*. are included [43].

304 The Zn concentrations of BT and MT are almost identical and together are significantly
305 elevated compared to 'normal' tissues ($p < 0.0001$), with BT ranging from 1.5 to 66.8 $\mu g\ g^{-1}$ with
306 a mean of 15.4 ± 16.2 $\mu g\ g^{-1}$ (SD), and MT ranging from 2.0 to 57.5 $\mu g\ g^{-1}$ with a mean of 15.2 ±
307 16.2 $\mu g\ g^{-1}$ (SD) (Table 1). Both BT and MT have significantly elevated Zn concentrations compared
308 to HT ($p = 0.00013$ and $p = 0.00012$, respectively) and NAT(MT) ($p < 0.0001$ for both), but not
309 NAT(BT) ($p = 0.32$ and $p = 0.39$, respectively) (Fig. 1). As was observed for the Zn concentrations,
310 the δ^{66}Zn of BT and MT are nearly identical and both are significantly lower than in 'normal'
311 tissues ($p = 0.0049$), with BT ranging from -0.58 to -0.06‰ with a mean of -0.32 ± 0.16‰ (SD),
312 and MT ranging from -0.66 to -0.05‰ with a mean of -0.37 ± 0.17‰ (SD) (Table 2). Malignant
313 tumours have significantly lower δ^{66}Zn than HT ($p = 0.017$), but BT compared to HT just failed to
314 reach significance ($p = 0.058$). The δ^{66}Zn of both MT and BT are significantly lower than in NAT(BT)
315 ($p = 0.011$ and $p = 0.045$, respectively), but not NAT(MT) ($p = 0.093$ and $p = 0.45$, respectively)
316 (Fig. 2). Whereas Zn concentrations and δ^{66}Zn do not significantly correlate in benign ($\rho = -0.30$,
317 $p = 0.26$) nor malignant breast tumours ($\rho = -0.21$, $p = 0.38$), benign and malignant tumours were
318 generally characterized by higher Zn concentrations and lower δ^{66}Zn compared to their
319 respective NATs (Fig. 3).
320

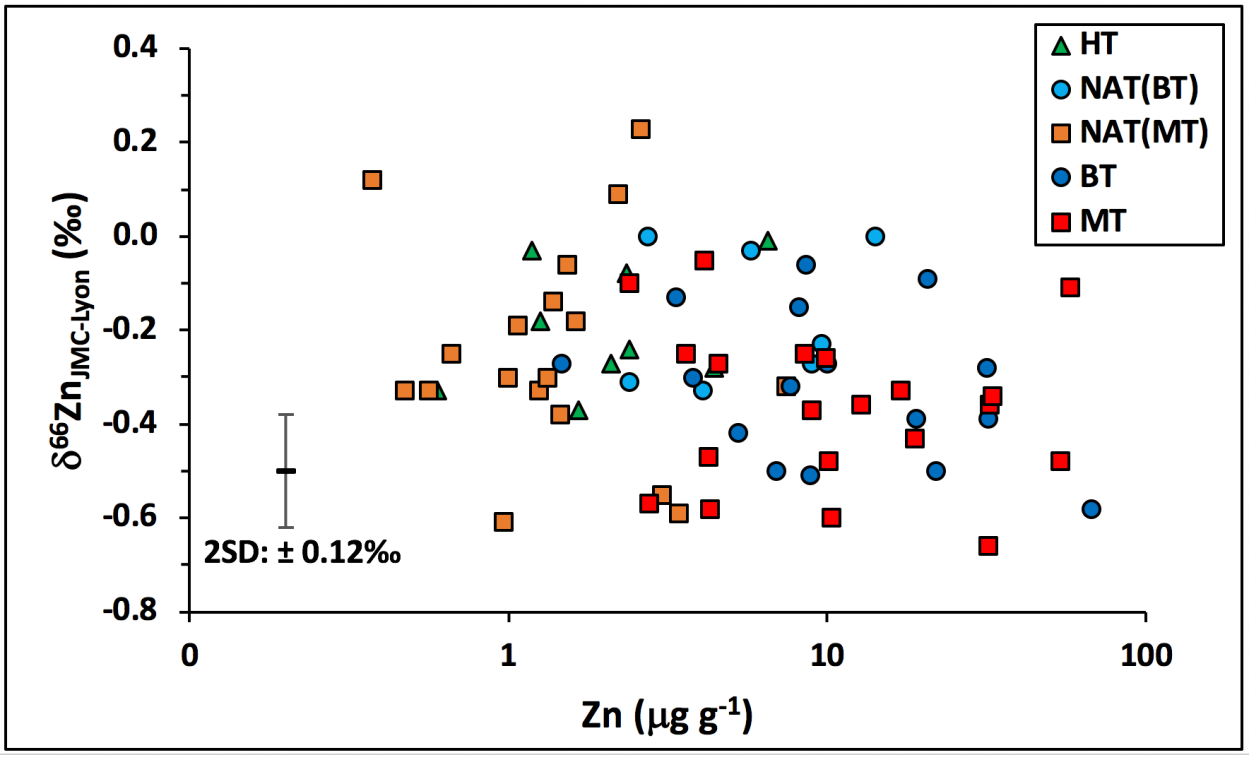

Figure 3 Relationship between δ^{66}Zn and Zn concentrations in healthy breast tissue taken during breast reduction surgery (HT); histologically normal tissue adjacent to benign tumour, NAT(BT); histologically normal tissue adjacent to malignant tumour, NAT(MT); benign tumour, BT; and malignant tumour, MT. Data from HT, NAT(MT), and MT measured by Larner *et al*. are included [43]. The error bar represents the between-run δ^{66}Zn reproducibility of ERM-BB184 (bovine muscle) achieved in this study.

Zinc concentrations and δ^{66}Zn in paired samples

Zinc concentrations were determined in five NAT(BT)-BT and 15 NAT(MT)-MT pairs (Table 1). As with the unpaired samples, no significant difference was found between the Zn levels of NAT(BT)-BT pairs (p = 0.44), whereby the benign tumours have Zn concentrations that only differ from paired tissue by 1.1 ± 3.9 μg g^{-1} (SD). In contrast, malignant tumours have Zn concentrations

that are significantly higher ($p < 0.0001$) compared to the paired adjacent tissue, with a mean concentration difference of 14.0 ± 14.3 μg g^{-1} (SD).

Zinc isotope data were obtained for four NAT(BT)-BT and 12 NAT(MT)-MT pairs (Table 2). In contrast to unpaired samples, the δ^{66}Zn of benign tumours do not significantly differ from their NAT(BT) counterparts ($p = 0.13$), with a mean difference of 0.10 ± 0.04‰ (SD). Similarly, malignant tumour δ^{66}Zn data are not significantly different from those of the paired adjacent tissue ($p = 0.18$), with a mean difference of 0.11 ± 0.25‰ (SD). The apparent differences in Zn isotope systematics of paired and unpaired samples may reflect that only a small number of paired samples were available for analysis.

Discussion

Distribution of Zn in NAT

Previously reported results in studies of breast tissue Zn levels vary greatly, with Zn concentrations in HT, NAT(MT), and MT spanning up to three orders of magnitude [47,60–66]. This could be due to a combination of breast tissue heterogeneity, the wide variety of analytical techniques employed, and some sample sets being prepared wet, dried to constant weight, or freeze-dried, making direct comparison challenging. However, the distribution of Zn appears to be fairly homogeneous in healthy breast tissue, whereas in tumours, hot spots occur where the amount of Zn is higher than elsewhere in the analyzed tissue [67]. In general, Zn concentrations in HT and NAT(MT) are significantly lower than in MT, which is in agreement with the results of this study. Interestingly, Zn concentrations in NAT(BT) are significantly elevated relative to HT

and NAT(MT) (Fig. 1). To the best of our knowledge, Zn concentrations in NAT(BT) were determined in just one other study [68], but there have been no direct comparisons of HT or NAT(MT) with NAT(BT). Although Zn concentrations were only able to be determined in eight NAT(BT) samples in this study, all eight possessed concentrations that are higher than the averages of HT and NAT(MT), indicating that an important relationship may have been identified.

There are several potential explanations for the increased Zn concentrations found in NAT(BT). Histologically normal tissue adjacent to benign tumours may contain a greater proportion of fibroglandular tissue compared to healthy breast tissue, which is primarily composed of lipid-rich adipose tissue [69]. Fibroglandular tissue is also denser than adipose tissue and could be a source of elevated Zn in histologically normal tissue adjacent to benign tumours [69]. Physiological processes that lead to increased Zn levels in benign or malignant tumours may have affected the composition of the healthy tissue margin around the lesions [47]. The regions immediately surrounding tumours have many morphologic and phenotypic distinctions from non-tumour-bearing healthy tissue, including pH levels, allelic imbalance and telomere length, stromal behaviour, and transcriptomic and epigenetic aberrations [70–73]. These phenotypic and genetic changes are apparent up to 4 cm away from tumour margins [46]. The high Zn concentrations in NAT(BT) compared to HT and NAT(MT) could also be associated with a specific immune response to a benign tumour. For example, a specific humoral immune response against benign tumours with a distinct serum reactivity pattern has been reported, and this seroreactivity is observed to decline with malignancy [74].

The approach of using NAT as a healthy control for cancer studies has many advantages. In particular it allows the comparison of samples from the same individual, which reduces

individual-specific and anatomical site-specific effects [46]. However, the results of this study and others suggests that NAT presents a unique intermediate, pre-neoplastic state between healthy and tumour tissue, which is composed of morphologically normal but molecularly altered cells [46–48,60–65,68]. Histological normalcy therefore does not necessarily imply biological normalcy, highlighting the potential need for changes to healthy control sampling practices for tissue samples adjacent to tumours [46]. By extension, it is also possible that even 'healthy' breast tissue taken during reduction mammoplasty is not truly representative of the normal condition. Breast size is correlated with factors such as body mass index, weight, height, and oral contraceptive use (hormone expression), and also specific genetic variants, that may influence Zn homeostasis [75,76].

Distribution of Zn in benign and malignant tumours

Malignant tumours contain significantly elevated levels of Zn compared to HT and NAT(MT) (Fig. 1), likely due to the increased expression of Zn importers (ZIP5, ZIP6, ZIP7, ZIP8, and ZIP10) in cancer cells [34,35]. The observation of malignant breast tumours containing elevated levels of Zn is consistent with previous results [47,60–65]. The δ^{66}Zn of MT are lower than in HT and NAT(MT) (Fig. 2), but interestingly, this only reached significance for HT. This selective distribution of Zn might be associated with specific mechanisms of Zn transport from NAT(MT) to MT mediated by the tumour or immune system, or it might be the result of defence mechanism 'exhaustion' in the surrounding tissue [77–79]. Of particular interest are the almost indistinguishable Zn concentrations (Fig. 1) and δ^{66}Zn (Fig. 2) found in BT and MT. As mentioned earlier, the direct comparison of breast tissue Zn concentrations between studies is a challenge,

but when both benign and malignant breast tumours have been analysed, Zn levels were consistently found to be similar [68,80–83]. Increased expression of ZIPs, ZnT2, and metallothionein in breast cancer cells is well-documented and results reported here indicate that their net isotopic product is an isotopically light Zn pool in breast cancer tumours [34,35,37,38]. Little is known about protein expression in benign breast tumours. However, there are reports of increased metallothionein-1 expression in malignant breast tissue compared to fibroadenomas [84]. This makes the similarities between the δ^{66}Zn of BT and MT even more intriguing as metallothionein has been suggested as the source of isotopically light Zn in malignant breast tumours [43]. A suitable mechanism is therefore required to explain the similarities between the δ^{66}Zn of BT and MT.

If similar ZIP and ZnT expression in BT and MT are assumed to explain the almost indistinguishable Zn concentrations found in these tissues, increased expression of metallothionein-1 in malignant breast tissue compared to fibroadenomas should give MT a lighter Zn isotopic composition than BT. The lack of a difference in δ^{66}Zn between BT and MT may possibly reflect the increased production of MMPs by breast cancer cells. Under normal physiological conditions, MMP activity is precisely regulated in order to prevent tissue disruption, but in cancer cells the physiological balance is disrupted, allowing tumour cells to invade adjacent healthy tissue [85]. In malignant breast tissue, MMP-1, -2, -8, -9, -10, -11, -12, -13, -15, -19, -23, -24, -27, and -28 are strongly expressed compared to normal breast tissue [85]. Similar to how the increased Zn of tumours is heterogeneously distributed, this also appears to apply to the distribution of MMPs [67]. This was been demonstrated for MMP-11, and also extends to its expression in metastatic specimens compared to non-metastatic tumour samples, which is

421 increased in the former [67,86]. A study of MMP-2 and MMP-9 found expression tended to be
422 significantly higher in malignant breast tissue compared to fibroadenomas [87]. Matrix
423 metalloproteinases exhibit considerable diversity in their domain structures and protein
424 substrate specificities, but Zn and cysteine residues are structural elements shared by all
425 members of the MMP family [40,88]. Furthermore, all members of the MMP gene family share
426 that they are synthesized in a latent, inactive form as a result of the formation of an
427 intramolecular complex between the single cysteine residue in its pro-peptide domain and the
428 essential Zn ion in the catalytic domain - a complex which blocks the active site [88]. The MMPs
429 in malignant breast tumours are predominantly in their latent form but can become activated by
430 the dissociation of the cysteine residue from the complex [89,90]. The activation of this so-called
431 'cysteine-switch' in MMPs mostly occurs outside of the cell once exposed to the extracellular
432 environment through the removal of their autoinhibitory pro-domain and changes the role of Zn
433 to the catalytic function [88,91,92]. However, MMPs including MMP-11 and -23 (strongly
434 expressed in breast cancer tissue) are activated by a pro-protein convertase within the secretory
435 pathway (Fig. 4) [93–97].

436 Activated MMPs are critical in the process of degrading various cell adhesion molecules
437 in ECM, thereby giving cancer cells access to new territories [42]. The core structure of a latent
438 MMP is $Zn(His)_3(Cys)^{2+}$ but when activated, the core structure becomes $Zn(His)_3(H_2O)^{2+}$. Density
439 functional theory estimates of Zn isotope fractionation suggest that the $\delta^{66}Zn$ of activated MMPs
440 should be 0.40‰ higher than for latent MMPs ($\Delta^{66}Zn_{\text{Activated MMP – Latent MMP}}$ = 0.40‰ at 310 K) and
441 even about 0.17‰ higher than for histidine [44]. Therefore, any light Zn isotope signature
442 imparted on MT by S-rich metallothionein may be compensated by the isotopically heavy Zn

associated with histidine from activated MMPs (Fig. 4). As such, this mechanism can potentially account for the Zn isotope similarities between BT and MT. Based on the available data, a potential Zn stable isotope biomarker (whether identified in serum, urine, or another reservoir) might indicate the presence of a breast tumour but may lack the ability to differentiate whether it is benign or malignant. Additionally, taking into account that Zn concentrations in tumours are affected by the microenvironment of surrounding tissue, our findings of significant differences in Zn concentrations of NAT(MT) and NAT(BT), despite similarity in BT and MT, support the assumption of physiological processes' dissimilarity in NAT(MT) and NAT(BT) [98].

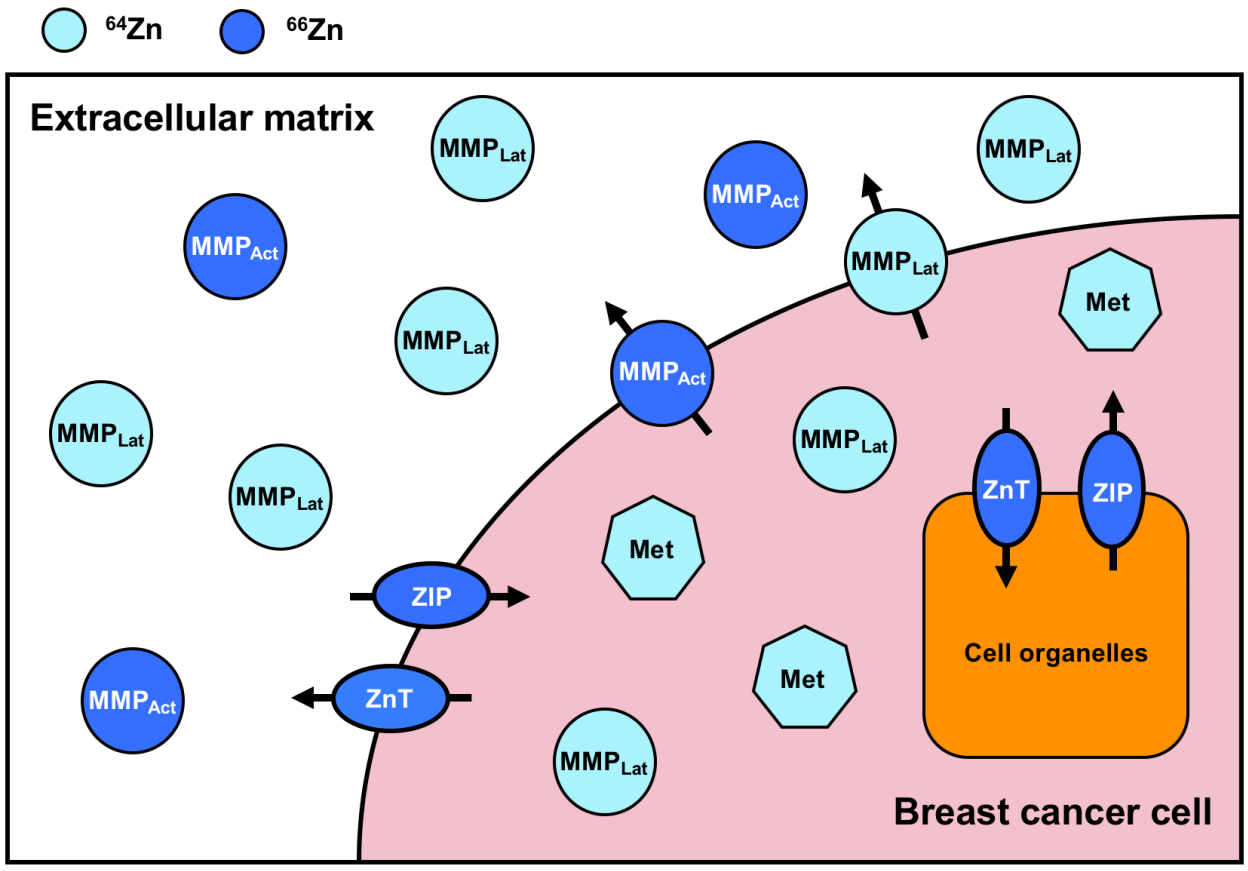

Figure 4 A schematic of Zn trafficking in and around a simplified breast cancer cell. Zinc in dark and light blue represents a relative enrichment in the heavy (^{66}Zn) and light (^{64}Zn) Zn isotope, respectively. ZIPs transport Zn into the cytoplasm both from outside the cell and from organelles. ZnTs transport Zn from the cytoplasm to both the cell organelles and outside of the cell. Metallothionein and MMPs (both activated and latent) are strongly expressed compared to in

457 healthy breast tissue and benign tumours. Abbreviations: latent matrix metalloproteinase,
458 MMP_{Lat} (light blue circles); activated matrix metalloproteinase, MMP_{Act} (dark blue circles);
459 metallothionein, Met (light blue heptagons); Zn-regulated transporter, Fe-regulated transporter-
460 like protein, ZIP; Zn transporter protein, ZnT (dark blue ellipses).
461

462 **Study limitations**

463 Limitations of this study include (1) the relatively small sample size; (2) sex - all patients
464 recruited for this study were female, so findings may only be applicable to female patients with
465 benign and malignant breast tumours; (3) the type, stage, and grade of tumours, as well as
466 differences in hormonal status, were not controlled for in the analysis as covariates; (4) age-
467 associated changes in Zn homeostasis: participant ages ranged from 21 to 84 years and were not
468 accounted for in the analysis (although, there does not appear to be an age effect for Zn
469 concentrations in breast cancer tissue); (5) samples were received from only one hospital which
470 could introduce selection bias due to the influence of race, cultural, and socioeconomic
471 background of participants and the types of tumours obtained; (6) patients had varied treatment
472 histories that might influence Zn concentrations and stable isotope compositions; and (7)
473 smoking and other environmental factors (including varying diets, breastfeeding) known to
474 influence Zn metabolism were not accounted for [99–103]. The results may therefore be
475 distorted, but the consistency of results between unpaired and paired samples (MT-NAT(MT) and
476 BT-NAT(BT)) indicates that these findings are unlikely to be due to non-tumour-related factors.
477 Moreover, the analysis of paired samples with the comparison of within-subject variability allows
478 controlling for age, medical history, and environmental factors that may influence the Zn
479 concentration and isotopic composition.
480

Future work

A key finding of Larner *et al*. was that the preferential sequestration of isotopically light Zn into breast cancer cells requires an isotopically heavy Zn pool to be present in the body to preserve the isotopic mass balance of the system [43]. However, no statistically significant difference in δ^{66}Zn was found between the blood serum of patients and controls. This may reflect the small mass of low-δ^{66}Zn that is sequestered in breast tumours and/or the rapid serum Zn turnover rate of over 150 times per day [104]. Further, recent work has found that an up to 25% decrease in serum Zn concentrations in the three hours postprandially (i.e. after eating) does not significantly fractionate serum Zn isotopes, which was hypothesized to be related to the rapid postprandial transfer of albumin-bound Zn in serum to the liver and pancreas to participate in phosphorylation reactions and the synthesis of digestive enzymes, respectively [57]. This suggests that a much larger source of effect than observed here (from the preferential accumulation of ^{64}Zn in benign and malignant breast tumours) is required to significantly alter the Zn isotopic composition of blood serum. However, the study of serum Zn isotopic compositions for breast cancer patients could benefit from analyses of additional samples as only a limited number were studied previously [43]. Within serum, the Zn-binding protein α-2-macroglobulin could be investigated to determine if it hosts the predicted isotopically heavy Zn pool. Zinc is bound more tightly by α-2-macroglobulin than albumin, which implies that the Zn isotope compositions of α-2-macroglobulin is more likely to reflect long-term disruptions to Zn homeostasis [105].

The preferential excretion of isotopically light Zn in the urine of PDAC patients compared to healthy controls demonstrates that Zn isotopes in urine may have potential as prognostic

503 and/or diagnostic markers of cancer [29]. Further, new work by Schilling *et al.* shows that there
504 is negligible difference in the δ^{66}Zn of urine from breast cancer patients and healthy controls (p
505 = 0.32) [106]. However, paradoxically, the disruption of Zn homeostasis in patients with benign
506 tumours is reflected in slightly higher urinary Zn concentrations (p = 0.12) and significantly lower
507 δ^{66}Zn (p = 0.03) relative to healthy controls. Opposite to what was expected given the higher Zn
508 concentrations and preferential uptake of ^{64}Zn by benign tumours compared to NAT and healthy
509 tissue, this represents an interesting basis for future work. With the caveat that the analysis of
510 additional samples is required, it is possible that urinary δ^{66}Zn may have the potential to non-
511 invasively indicate whether a breast lump is benign or malignant.

512 The results presented here demonstrate that further studies characterising differences in
513 Zn levels, isotopic compositions, and mechanisms that alter gene expression and tumour-
514 adjacent stroma in NAT and healthy breast tissue are needed to gain a better understanding of
515 the healthy condition [46]. Such studies should be conducted on samples that have been freeze-
516 dried with the wet weight recorded to allow comparison of concentrations with previously
517 published results. Investigations that target the concentrations and isotopic compositions of
518 further relevant elements, such as Cu and Fe, are also desirable as they may provide further
519 insights into additional homeostatic changes that occur in tissue adjacent to tumours. It might
520 also be beneficial for cancer prevention and therapy, as well as prognosis assessment, to
521 understand the difference in Zn-related processes between NAT(MT) and NAT(BT), and their
522 influence on disease progression. Additional malignant breast tumour samples of varied grade,
523 stage, type, and hormonal status are also needed to properly evaluate potential associations
524 between hormonal status, tumour characteristics, and Zn concentrations, in addition to δ^{66}Zn.

525 Zinc stable isotope compositions have the potential to offer insights into the underlying
526 processes leading to observed trends in Zn accumulation. Taken together, such work may lead to
527 novel therapeutic strategies in the treatment of cancer if key differences are discovered between
528 the tissues [46].

529 Costello *et al*. identified decreased levels of Zn in ductal malignant cells compared to
530 normal ductal epithelium [107]. These results (produced using a semi-quantitative dithizone
531 staining technique) potentially conflict with the growing body of work that has reported the
532 enrichment of Zn in breast cancer tissues compared to adjacent histologically normal tissue
533 [46,47,60–65,68]. In cancerous tissues, cancer cells are often mixed with connective tissue,
534 immune cells, and stromal tissues [108]. If the elevated Zn in breast cancer tissues is not
535 associated with breast cancer cells, as conventionally understood, it will be important to identify
536 where Zn is localized at the cellular level. Recently, Zn concentrations have been compared in
537 cancer cell clusters and adjacent stroma, but future work should employ single-cell laser ablation
538 (LA)-ICP-MS for an *in-situ* quantitative assessment of Zn concentrations in individual cells
539 [65,109–111]. If the results of Costello *et al*. are reproduced, these observations may transform
540 the way Zn dyshomeostasis in breast cancer is currently understood [107].

541

542 **Conclusions**

543 This study examined the disruption of Zn homeostasis associated with benign breast
544 disease and breast cancer. Notably, this is the first instance of a comparison of Zn concentrations
545 and δ^{66}Zn in the three "healthy" tissue types, HT, NAT(BT), and NAT(MT), as well as both BT and

546 MT. Zinc concentrations in NAT(BT) are significantly elevated relative to HT and NAT(MT),
547 possibly due to a specific immune response to benign tumours [74]. Histologically normal tissue
548 adjacent to tumours commonly serves as a healthy control sample for cancer studies. These
549 findings call into question the assumption that histological normalcy implies biological normalcy,
550 and suggest the potential need for changes to healthy control sampling practices. Higher Zn
551 concentrations in NAT(BT) compared to NAT(MT) requires further investigation as a possible
552 marker of malignization and disease prognosis.

553 Malignant tumours contain significantly elevated levels of Zn compared to HT and
554 NAT(MT) (Fig. 1), likely due to the increased expression of Zn importers (ZIP5, ZIP6, ZIP7, ZIP8,
555 and ZIP10) in cancer cells [34,35]. The δ^{66}Zn of MT are lower than in HT and NAT(MT) (Fig. 2), but
556 this only reached significance for HT. Of particular interest are the almost indistinguishable Zn
557 concentrations (Fig. 1) and δ^{66}Zn (Fig. 2) found in BT and MT. There is little documentation of ZIP
558 and ZnT expression in benign tumours, but metallothionein-1 is overexpressed in MT compared
559 to fibroadenomas and should, in theory, lead to a δ^{66}Zn in MT that is lower than in BT [84]. It is
560 possible that the lack of a difference in δ^{66}Zn between BT and MT may reflect the increased
561 production of MMPs by breast cancer cells, as this could compensate for the isotopically light
562 signature of metallothionein-bound Zn (Fig. 4) [85]. A Zn isotope biomarker (whether identified
563 in serum, urine, or another reservoir) might have the potential to identify the presence of a breast
564 tumour, but similarities between bulk tissue Zn concentrations and δ^{66}Zn in the two pathologies
565 suggests such a biomarker may lack the ability to differentiate whether the tumour is benign or
566 malignant. These findings are preliminary, and additional studies are required to establish the
567 features of Zn dyshomeostasis in benign tumours, breast cancer, and adjacent tissues.

Acknowledgements

This study was supported by the National Institute for Health Research Imperial Biomedical Research Centre, the Imperial Experimental Cancer Medicine Centre, and the Cancer Research UK Imperial Centre at Imperial College London. The collaboration between Queen's University and Imperial College London was made possible through the support of the Kimberley Foundation Hugh C. Morris Experiential Learning Fellowship of KVS. RM was supported by a Janet Watson Scholarship. Support for MC was provided by Science and Solutions for a Changing Planet DTP and the Natural Environment Research Council [NE/S007415/1]. KS was supported by the Fell Fund of the University of Oxford. FL thanks the Department of Earth Sciences at the University of Oxford for the internal funding that contributed to the completion of this research. Thank you to Alan (Yu-Te) Hsieh of the University of Oxford Department of Earth Sciences for his assistance with MC-ICP-MS operation and maintenance. KS is grateful to Frank Vanhaecke, Peir Pufahl, Christopher Spencer, and Scott Lamoureux for their helpful comments.

Conflicts of Interest

There are no conflicts to declare.

Data availability statement

The data underlying this article are available in the article and in its online supplementary material.

590 **References**

591

592 1. Vašák M, Hasler DW. Metallothioneins: new functional and structural insights. *Current*
593 *Opinion in Chemical Biology* 2000;**4**:177–83.

594 2. Andreini C, Banci L, Bertini I *et al.* Counting the Zinc-Proteins Encoded in the Human Genome.
595 *Journal of Proteome Research* 2006;**5**:196–201.

596 3. Truong-Tran AQ, Carter J, Ruffin R *et al.* New insights into the role of zinc in the respiratory
597 epithelium. *Immunology & Cell Biology* 2001;**79**:170–7.

598 4. Haase H, Rink L. Multiple impacts of zinc on immune function. *Metallomics* 2014;**6**:1175–80.

599 5. Rink L. Zinc and the immune system. *Proceedings of the Nutrition Society* 2000;**59**:541–52.

600 6. Wellenreuther G, Cianci M, Tucoulou R *et al.* The ligand environment of zinc stored in
601 vesicles. *Biochemical and Biophysical Research Communications* 2009;**380**:198–203.

602 7. Sandstead HH, Smith Jr JC. Deliberations and evaluations of approaches, endpoints and
603 paradigms for determining zinc dietary recommendations. *The Journal of Nutrition*
604 1996;**126**:2410S-2418S.

605 8. Institute of Medicine (US) Panel on Micronutrients. *Dietary Reference Intakes for Vitamin A,*
606 *Vitamin K, Arsenic, Boron, Chromium, Copper, Iodine, Iron, Manganese, Molybdenum, Nickel,*
607 *Silicon, Vanadium, and Zinc*. Washington (DC): National Academies Press (US), 2001.

608 9. Albarède F, Télouk P, Balter V. Medical Applications of Isotope Metallomics. *Reviews in*
609 *Mineralogy and Geochemistry* 2017;**82**:851–85.

610 10. Halicz L, Galy A, Belshaw NS *et al.* High-precision measurement of calcium isotopes in
611 carbonates and related materials by multiple collector inductively coupled plasma mass
612 spectrometry (MC-ICP-MS). *Journal of Analytical Atomic Spectrometry* 1999;**14**:1835–8.

613 11. Maréchal CN, Télouk P, Albarède F. Precise analysis of copper and zinc isotopic
614 compositions by plasma-source mass spectrometry. *Chemical Geology* 1999;**156**:251–73.

615 12. Sauzéat L, Bernard E, Perret-Liaudet A *et al.* Isotopic evidence for disrupted copper
616 metabolism in amyotrophic lateral sclerosis. *iScience* 2018;**6**:264–71.

617 13. Moynier F, Foriel J, Shaw AS *et al.* Distribution of Zn isotopes during Alzheimer's disease.
618 *Geochemical Perspective Letters* 2017;**3**:142–50.

619 14. Lauwens S, Costas-Rodríguez M, Vlierberghe HV *et al.* Cu isotopic signature in blood serum
620 of liver transplant patients: a follow-up study. *Scientific Reports* 2016;**6**:30683.

15. Balter V, da Costa AN, Bondanese VP *et al.* Natural variations of copper and sulfur stable isotopes in blood of hepatocellular carcinoma patients. *Proceedings of the National Academy of Sciences of the United States of America* 2015;**112**:982–5.

16. Costas-Rodríguez M, Anoshkina Y, Lauwens S *et al.* Isotopic analysis of Cu in blood serum by multi-collector ICP-mass spectrometry: a new approach for the diagnosis and prognosis of liver cirrhosis? *Metallomics* 2015;**7**:491–8.

17. Télouk P, Puisieux A, Fujii T *et al.* Copper isotope effect in serum of cancer patients. A pilot study. *Metallomics* 2015;**7**:299–308.

18. Aramendía M, Rello L, Resano M *et al.* Isotopic analysis of Cu in serum samples for diagnosis of Wilson's disease: a pilot study. *Journal of Analytical Atomic Spectrometry* 2013;**28**:675–81.

19. Resano M, Aramendía M, Rello L *et al.* Direct determination of Cu isotope ratios in dried urine spots by means of fs-LA-MC-ICPMS. Potential to diagnose Wilson's disease. *Journal of Analytical Atomic Spectrometry* 2013;**28**:98–106.

20. Hastuti AAMB, Costas-Rodríguez M, Matsunaga A *et al.* Cu and Zn isotope ratio variations in plasma for survival prediction in hematological malignancy cases. *Scientific Reports* 2020;**10**:1–12.

21. Moynier F, Creech J, Dallas J *et al.* Serum and brain natural copper stable isotopes in a mouse model of Alzheimer's disease. *Scientific Reports* 2019;**9**:1–7.

22. Moynier F, Borgne ML, Laoud E *et al.* Copper and zinc isotopic excursions in the human brain affected by Alzheimer's disease. *Alzheimer's & Dementia: Diagnosis, Assessment & Disease Monitoring* 2020;**12**:e12112.

23. Toubhans B, Gourlan AT, Telouk P *et al.* Cu isotope ratios are meaningful in ovarian cancer diagnosis. *Journal of Trace Elements in Medicine and Biology* 2020;**62**:126611.

24. Zhang J, Li J, Zhang L *et al.* Precise determination of the molybdenum isotopic composition of urine by multiple collector inductively coupled plasma mass spectrometry. *Rapid Communications in Mass Spectrometry* 2020;**34**:e8658.

25. Albarède F, Telouk P, Lamboux A *et al.* Isotopic evidence of unaccounted for Fe and Cu erythropoietic pathways. *Metallomics* 2011;**3**:926–33.

26. Van Heghe L, Engström E, Rodushkin I *et al.* Isotopic analysis of the metabolically relevant transition metals Cu, Fe and Zn in human blood from vegetarians and omnivores using multi-collector ICP-mass spectrometry. *Journal of Analytical Atomic Spectrometry* 2012;**27**:1327–34.

27. Van Heghe L, Deltombe O, Delanghe J *et al.* The influence of menstrual blood loss and age on the isotopic composition of Cu, Fe and Zn in human whole blood. *Journal of Analytical Atomic Spectrometry* 2014;**29**:478–82.

28. Eisenhauer A, Müller M, Heuser A *et al.* Calcium isotope ratios in blood and urine: A new biomarker for the diagnosis of osteoporosis. *Bone Reports* 2019:100200.

29. Schilling K, Larner F, Saad A *et al.* Urine metallomics signature as an indicator of pancreatic cancer. *Metallomics* 2020;**12**:752–7.

30. Moore RE, Rehkämper M, Maret W *et al.* Assessment of coupled Zn concentration and natural stable isotope analyses of urine as a novel probe of Zn status. *Metallomics* 2019;**11**:1506–17.

31. Heuser A, Frings-Meuthen P, Rittweger J *et al.* Calcium Isotopes in Human Urine as a Diagnostic Tool for Bone Loss: Additional Evidence for Time Delays in Bone Response to Experimental Bed Rest. *Frontiers in Physiology* 2019;**10**:12.

32. Costas-Rodríguez M, Van Heghe L, Vanhaecke F. Evidence for a possible dietary effect on the isotopic composition of Zn in blood via isotopic analysis of food products by multi-collector ICP-mass spectrometry. *Metallomics* 2014;**6**:139–46.

33. Jaouen K, Balter V. Menopause effect on blood Fe and Cu isotope compositions: Menopause Effect on Blood Fe and Cu Isotopes. *American Journal of Physical Anthropology* 2014;**153**:280–5.

34. Taylor KM, Morgan HE, Smart K *et al.* The Emerging Role of the LIV-1 Subfamily of Zinc Transporters in Breast Cancer. *Molecular Medicine* 2007;**13**:396–406.

35. Kelleher SL, Seo YA, Lopez V. Mammary gland zinc metabolism: regulation and dysregulation. *Genes & Nutrition* 2009;**4**:83–94.

36. Chasapis CT, Loutsidou AC, Spiliopoulou CA *et al.* Zinc and human health: an update. *Archives of Toxicology* 2012;**86**:521–34.

37. Lopez V, Foolad F, Kelleher SL. ZnT2-overexpression represses the cytotoxic effects of zinc hyper-accumulation in malignant metallothionein-null T47D breast tumor cells. *Cancer Letters* 2011;**304**:41–51.

38. Alam S, Kelleher SL. Cellular Mechanisms of Zinc Dysregulation: A Perspective on Zinc Homeostasis as an Etiological Factor in the Development and Progression of Breast Cancer. *Nutrients* 2012;**4**:875–903.

39. Pan Z, Choi S, Ouadid-Ahidouch H *et al.* Zinc transporters and dysregulated channels in cancers. *Frontiers in Bioscience (Landmark edition)* 2017;**22**:623–43.

40. Holanda AO do N, Oliveira ARS de, Cruz KJC *et al.* Zinc and metalloproteinases 2 and 9: What is their relation with breast cancer? *Revista da Associação Médica Brasileira* 2017;**63**:78–84.

687 41. Cox G, Steward WP, O'Byrne KJ. The plasmin cascade and matrix metalloproteinases in non-
688 small cell lung cancer. *Thorax* 1999;**54**:169–79.

689 42. Gialeli C, Theocharis AD, Karamanos NK. Roles of matrix metalloproteinases in cancer
690 progression and their pharmacological targeting: MMPs as potential targets in malignancy. *FEBS*
691 *Journal* 2011;**278**:16–27.

692 43. Larner F, N. Woodley L, Shousha S *et al.* Zinc isotopic compositions of breast cancer tissue.
693 *Metallomics* 2015;**7**:112–7.

694 44. Fujii T, Moynier F, Blichert-Toft J *et al.* Density functional theory estimation of isotope
695 fractionation of Fe, Ni, Cu, and Zn among species relevant to geochemical and biological
696 environments. *Geochimica et Cosmochimica Acta* 2014;**140**:553–76.

697 45. Cui Y, Vogt S, Olson N *et al.* Levels of Zinc, Selenium, Calcium, and Iron in Benign Breast
698 Tissue and Risk of Subsequent Breast Cancer. *Cancer Epidemiology and Prevention Biomarkers*
699 2007;**16**:1682–5.

700 46. Aran D, Camarda R, Odegaard J *et al.* Comprehensive analysis of normal adjacent to tumor
701 transcriptomes. *Nature Communications* 2017;**8**:1–14.

702 47. Geraki K, Farquharson MJ, Bradley DA. Concentrations of Fe, Cu and Zn in breast tissue: a
703 synchrotron XRF study. *Physics in Medicine & Biology* 2002;**47**:2327.

704 48. Slaughter DP, Southwick HW, Smejkal W. "Field cancerization" in oral stratified squamous
705 epithelium. Clinical implications of multicentric origin. *Cancer* 1953;**6**:963–8.

706 49. Moore RET, Larner F, Coles BJ *et al.* High Precision Zinc Stable Isotope Measurement of
707 Certified Biological Reference Materials Using the Double Spike Technique and Multiple
708 Collector-ICP-MS. *Analytical and Bioanalytical Chemistry* 2017;**409**:2941–50.

709 50. Bridgestock LJ, Williams H, Rehkämper M *et al.* Unlocking the zinc isotope systematics of
710 iron meteorites. *Earth and Planetary Science Letters* 2014;**400**:153–64.

711 51. Arnold T, Schönbächler M, Rehkämper M *et al.* Measurement of zinc stable isotope ratios in
712 biogeochemical matrices by double-spike MC-ICPMS and determination of the isotope ratio
713 pool available for plants from soil. *Analytical and Bioanalytical Chemistry* 2010;**398**:3115–25.

714 52. Archer C, B. Andersen M, Cloquet C *et al.* Inter-calibration of a proposed new primary
715 reference standard AA-ETH Zn for zinc isotopic analysis. *Journal of Analytical Atomic*
716 *Spectrometry* 2017;**32**:415–9.

717 53. Cloquet C, Carignan J, Lehmann MF *et al.* Variation in the isotopic composition of zinc in the
718 natural environment and the use of zinc isotopes in biogeosciences: a review. *Analytical and*
719 *Bioanalytical Chemistry* 2008;**390**:451–63.

720 54. Larner F, Rehkämper M. Evaluation of Stable Isotope Tracing for ZnO Nanomaterials□New
721 Constraints from High Precision Isotope Analyses and Modeling. *Environmental Science &*
722 *Technology* 2012;**46**:4149–58.

723 55. Siebert C, Nägler TF, Kramers JD. Determination of molybdenum isotope fractionation by
724 double-spike multicollector inductively coupled plasma mass spectrometry. *Geochemistry,*
725 *Geophysics, Geosystems* 2001;**2**.

726 56. Moeller K, Schoenberg R, Pedersen R-B *et al.* Calibration of the New Certified Reference
727 Materials ERM-AE633 and ERM-AE647 for Copper and IRMM-3702 for Zinc Isotope Amount
728 Ratio Determinations. *Geostandards and Geoanalytical Research* 2012;**36**:177–99.

729 57. Sullivan K, Moore RET, Rehkämper M *et al.* Postprandial zinc stable isotope response in
730 human blood serum. *Metallomics* 2020;**9**:1380–8.

731 58. Ellis IO, Galea M, Broughton N *et al.* Pathological prognostic factors in breast cancer. II.
732 Histological type. Relationship with survival in a large study with long-term follow-up.
733 *Histopathology* 1992;**20**:479–89.

734 59. Alkabban FM, Ferguson T. Breast Cancer. *Breast Cancer*. StatPearls Publishing, 2020.

735 60. Raju GJN, Sarita P, Kumar MR *et al.* Trace elemental correlation study in malignant and
736 normal breast tissue by PIXE technique. *Nuclear Instruments and Methods in Physics Research*
737 *Section B: Beam Interactions with Materials and Atoms* 2006;**247**:361–7.

738 61. Ionescu JG, Novotny J, Stejskal V *et al.* Increased levels of transition metals in breast cancer
739 tissue. *Neuro Endocrinology Letters* 2006;**27**:36–9.

740 62. Millos J, Costas-Rodríguez M, Lavilla I *et al.* Multiple small volume microwave-assisted
741 digestions using conventional equipment for multielemental analysis of human breast biopsies
742 by inductively coupled plasma optical emission spectrometry. *Talanta* 2009;**77**:1490–6.

743 63. Millos J, Costas-Rodríguez M, Lavilla I *et al.* Multielemental determination in breast
744 cancerous and non-cancerous biopsies by inductively coupled plasma-mass spectrometry
745 following small volume microwave-assisted digestion. *Analytica Chimica Acta* 2008;**622**:77–84.

746 64. Riesop D, Hirner AV, Rusch P *et al.* Zinc distribution within breast cancer tissue: A possible
747 marker for histological grading? *Journal of Cancer Research and Clinical Oncology*
748 2015;**141**:1321–31.

749 65. Rusch P, Hirner AV, Schmitz O *et al.* Zinc distribution within breast cancer tissue of different
750 intrinsic subtypes. *Archives of Gynecology and Obstetrics* 2020:1–11.

751 66. Geraki K, Farquharson MJ, Bradley DA *et al.* A synchrotron XRF study on trace elements and
752 potassium in breast tissue. *Nuclear Instruments and Methods in Physics Research Section B:*
753 *Beam Interactions with Materials and Atoms* 2004;**213**:564–8.

754 67. González de Vega R, Sanchez MLF, Eiro N *et al.* Multimodal laser ablation/desorption
755 imaging analysis of Zn and MMP-11 in breast tissues. *Analytical and Bioanalytical Chemistry*
756 2018;**410**:913–22.

757 68. Siddiqui MKJ, Jyoti, Singh S *et al.* Comparison of some trace elements concentration in
758 blood, tumor free breast and tumor tissues of women with benign and malignant breast
759 lesions: An Indian study. *Environment International* 2006;**32**:630–7.

760 69. Sun X, Sandhu R, Figueroa JD *et al.* Benign Breast Tissue Composition in Breast Cancer
761 Patients: Association with Risk Factors, Clinical Variables, and Gene Expression. *Cancer*
762 *Epidemiology Biomarkers & Prevention* 2014;**23**:2810–8.

763 70. Heaphy CM, Griffith JK, Bisoffi M. Mammary field cancerization: molecular evidence and
764 clinical importance. *Breast Cancer Research and Treatment* 2009;**118**:229–39.

765 71. Heaphy CM, Bisoffi M, Fordyce CA *et al.* Telomere DNA content and allelic imbalance
766 demonstrate field cancerization in histologically normal tissue adjacent to breast tumors.
767 *International Journal of Cancer* 2006;**119**:108–16.

768 72. Trujillo KA, Heaphy CM, Mai M *et al.* Markers of fibrosis and epithelial to mesenchymal
769 transition demonstrate field cancerization in histologically normal tissue adjacent to breast
770 tumors. *International Journal of Cancer* 2011;**129**:1310–21.

771 73. Gerweck LE, Seetharaman K. Cellular pH gradient in tumor versus normal tissue: potential
772 exploitation for the treatment of cancer. *Cancer Research* 1996;**56**:1194–8.

773 74. Comtesse N, Zippel A, Walle S *et al.* Complex humoral immune response against a benign
774 tumor: Frequent antibody response against specific antigens as diagnostic targets. *Proceedings*
775 *of the National Academy of Sciences of the United States of America* 2005;**102**:9601–6.

776 75. Jemström H, Olsson H. Breast size in relation to endogenous hormone levels, body
777 constitution, and oral contraceptive use in healthy nulligravid women aged 19–25 years.
778 *American Journal of Epidemiology* 1997;**145**:571–80.

779 76. Eriksson N, Benton GM, Do CB *et al.* Genetic variants associated with breast size also
780 influence breast cancer risk. *BMC Medical Genetics* 2012;**13**:53.

781 77. Skrajnowska D, Bobrowska-Korczak B. Role of zinc in immune system and anti-cancer
782 defense mechanisms. *Nutrients* 2019;**11**:2273.

783 78. Kit OI, Zlatnik EY, Peredreyeva LV. Antiproliferative activity of zinc and metal alloy
784 nanoparticles in transplanted sarcomas. *Bulletin of Experimental Biology and Medicine*
785 2014;**156**:389–92.

786 79. Hashemi M, Ghavami S, Eshraghi M *et al.* Cytotoxic effects of intra and extracellular zinc
787 chelation on human breast cancer cells. *European Journal of Pharmacology* 2007;**557**:9–19.

80. Kanias GD, Kouri E, Arvaniti H *et al.* Trace element content in breasts with fibrocystic disease. *Biological Trace Element Research* 1994;**43**:363–70.

81. Majewska U, Banaś D, Braziewicz J *et al.* Trace element concentration distributions in breast, lung and colon tissues. *Physics in Medicine and Biology* 2007;**52**:3895–911.

82. Kubala-Kukuś A, Banaś D, Braziewicz J *et al.* Analysis of elemental concentration censored distributions in breast malignant and breast benign neoplasm tissues. *Spectrochimica Acta Part B: Atomic Spectroscopy* 2007;**62**:695–701.

83. Pasha Q, Malik SA, Iqbal J *et al.* Comparative Evaluation of Trace Metal Distribution and Correlation in Human Malignant and Benign Breast Tissues. *Biological Trace Element Research* 2008;**125**:30–40.

84. Sampaio FA, Martins LM, Dourado CS de ME *et al.* A case-control study of Metallothionein-1 expression in breast cancer and breast fibroadenoma. *Scientific Reports* 2019;**9**:1–5.

85. Köhrmann A, Kammerer U, Kapp M *et al.* Expression of matrix metalloproteinases (MMPs) in primary human breast cancer and breast cancer cell lines: New findings and review of the literature. *BMC Cancer* 2009;**9**:188.

86. González de Vega R, Clases D, Fernández-Sánchez ML *et al.* MMP-11 as a biomarker for metastatic breast cancer by immunohistochemical-assisted imaging mass spectrometry. *Analytical and Bioanalytical Chemistry* 2019;**411**:639–46.

87. Martins LM, de Melo Escorcio Dourado CS, Campos-Verdes LM *et al.* Expression of matrix metalloproteinase 2 and 9 in breast cancer and breast fibroadenoma: a randomized, double-blind study. *Oncotarget* 2019;**10**:6879–84.

88. Van Wart HE, Birkedal-Hansen H. The cysteine switch: a principle of regulation of metalloproteinase activity with potential applicability to the entire matrix metalloproteinase gene family. *Proceedings of the National Academy of Sciences of the United States of America* 1990;**87**:5578–82.

89. Candrea E, Senila S, Tatomir C *et al.* Active and inactive forms of matrix metalloproteinases 2 and 9 in cutaneous melanoma. *International Journal of Dermatology* 2014;**53**:575–80.

90. Sik Lee K, Young Rha S, Joong Kim S *et al.* Sequential activation and production of matrix metalloproteinase-2 during breast cancer progression. *Clinical & Experimental Metastasis* 1996;**14**:512–9.

91. Sternlicht MD, Werb Z. How matrix metalloproteinases regulate cell behavior. *Annual Review of Cell and Developmental Biology* 2001;**17**:463–516.

92. Austin KM, Covic L, Kuliopulos A. Matrix metalloproteases and PAR1 activation. *Blood* 2013;**121**:431–9.

93. Sato H, Kinoshita T, Takino T *et al.* Activation of a recombinant membrane type 1-matrix metalloproteinase (MT1-MMP) by furin and its interaction with tissue inhibitor of metalloproteinases (TIMP)-2. *FEBS Letters* 1996;**393**:101–4.

94. Wang X, Pei D. Shedding of Membrane Type Matrix Metalloproteinase 5 by a Furin-type Convertase. *Journal of Biological Chemistry* 2001;**276**:35953–60.

95. Kang T, Nagase H, Pei D. Activation of membrane-type matrix metalloproteinase 3 zymogen by the proprotein convertase furin in the trans-Golgi network. *Cancer Research* 2002;**62**:675–81.

96. Pei D, Weiss SJ. Furin-dependent intracellular activation of the human stromelysin-3 zymogen. *Nature* 1995;**375**:244–7.

97. Somerville RP, Oblander SA, Apte SS. Matrix metalloproteinases: old dogs with new tricks. *Genome Biology* 2003;**4**:216.

98. Murakami M, Hirano T. Intracellular zinc homeostasis and zinc signaling. *Cancer Science* 2008;**99**:1515–22.

99. Mirji S, Badiger NM, Sanyal K *et al.* Determination of trace elements in normal and malignant breast tissues of different age group using total reflection X-ray fluorescence spectrometer. *X-Ray Spectrometry* 2018;**47**:432–40.

100. Rishi I, Baidouri H, Abbasi JA *et al.* Prostate cancer in African American men is associated with downregulation of zinc transporters. *Applied Immunohistochemistry & Molecular Morphology* 2003;**11**:253–60.

101. Shoemaker ML, White MC, Wu M *et al.* Differences in breast cancer incidence among young women aged 20–49 years by stage and tumor characteristics, age, race, and ethnicity, 2004–2013. *Breast Cancer Research and Treatment* 2018;**169**:595–606.

102. Phillips DH, Venitt S. DNA and protein adducts in human tissues resulting from exposure to tobacco smoke. *International Journal of Cancer* 2012;**131**:2733–53.

103. Lönnerdal B. Trace element transport in the mammary gland. *Annual Review of Nutrition* 2007;**27**:165–77.

104. King JC, Shames DM, Woodhouse LR. Zinc Homeostasis in Humans. *The Journal of Nutrition* 2000;**130**:1360S-1366S.

105. Scott BJ, Bradwell AR. Identification of the serum binding proteins for iron, zinc, cadmium, nickel, and calcium. *Clinical Chemistry* 1983;**29**:629–33.

106. Schilling K, Moore RET, Sullivan KV *et al.* Zinc stable isotopes in urine as diagnostic for cancer of secretory organs. *Metallomics* 2021, DOI: 10.1093/mtomcs/mfab020.

855 107. Costello LC, Zou J, Franklin RB. In situ clinical evidence that zinc levels are decreased in
856 breast invasive ductal carcinoma. *Cancer Causes Control* 2016;**27**:729–35.

857 108. Morin RD, Montgomery SB. Chapter 3 - Cancer Transcriptome Sequencing and Analysis.
858 *Cancer Genomics*. Boston: Academic Press, 2014, 31–47.

859 109. Löhr K, Traub H, Jutta Wanka A *et al.* Quantification of metals in single cells by LA-ICP-MS:
860 comparison of single spot analysis and imaging. *Journal of Analytical Atomic Spectrometry*
861 2018;**33**:1579–87.

862 110. Van Malderen SJ, Vergucht E, De Rijcke M *et al.* Quantitative determination and subcellular
863 imaging of Cu in single cells via laser ablation-ICP-mass spectrometry using high-density
864 microarray gelatin standards. *Analytical Chemistry* 2016;**88**:5783–9.

865 111. Van Acker T, Buckle T, Van Malderen SJ *et al.* High-resolution imaging and single-cell
866 analysis via laser ablation-inductively coupled plasma-mass spectrometry for the determination
867 of membranous receptor expression levels in breast cancer cell lines using receptor-specific
868 hybrid tracers. *Analytica Chimica Acta* 2019;**1074**:43–53.

869
870
871
872
873
874
875
876
877
878
879
880
881
882
883
884
885
886
887
888
889
890
891
892
893
894

Table 1 Results for Zn concentrations (μg g^{-1}) measured in participant samples

Description	Mean (SD)	*n*	SE	Median	Range
HT	2.3 (1.7)	11	0.5	1.7	0.6 to 6.5
NAT(BT)	7.4 (4.4)	8	1.5	7.3	2.4 to 14.0
NAT(MT)	1.9 (1.6)	19	0.4	1.4	0.4 to 7.4
BT	15.4 (16.2)	17	3.9	8.5	1.5 to 66.8
MT	15.2 (16.2)	22	3.5	9.4	2.0 to 57.5
BT-NAT(BT) pair difference	1.1 (3.9)	5	1.7		
MT-NAT(MT) pair difference	14.0 (14.3)	15	3.7		

Standard deviation (SD) of values provided in brackets, ( ); *n* = number of samples/pairs; SE = standard error of the mean; HT = 'healthy' breast tissue taken during reduction mammoplasty; NAT(BT) = histologically normal tissue adjacent to benign tumour; NAT(MT) = histologically normal tissue adjacent to malignant tumour; BT = benign tumour; MT = malignant tumour. Paired sample statistics for BT-NAT(BT) and MT-NAT(MT) calculated based on differences in Zn concentration.

Table 2 Results for Zn isotope compositions ($\delta^{66}Zn_{JMC\text{-}Lyon}$, ‰) measured in participant samples

Description	Mean (SD)	*n*	SE	Median	Range
HT	-0.20 (0.13)	9	0.04	-0.24	-0.37 to -0.01
NAT(BT)	-0.17 (0.15)	7	0.06	-0.23	-0.33 to 0.00
NAT(MT)	-0.25 (0.23)	18	0.05	-0.30	-0.61 to 0.23
BT	-0.32 (0.16)	16	0.04	-0.31	-0.58 to -0.06
MT	-0.37 (0.17)	20	0.04	-0.36	-0.66 to -0.05
BT-NAT(BT) pair difference	-0.10 (0.04)	4	0.02		
MT-NAT(MT) pair difference	-0.11 (0.25)	12	0.07		

Standard deviation (SD) of values provided in brackets, ( ); *n* = number of samples/pairs; SE = standard error of the mean; HT = 'healthy' breast tissue taken during reduction mammoplasty; NAT(BT) = histologically normal tissue adjacent to benign tumour; NAT(MT) = histologically normal tissue adjacent to malignant tumour; BT = benign tumour; MT = malignant tumour. Paired sample statistics for BT-NAT(BT) and MT-NAT(MT) calculated based on differences in $\delta^{66}Zn$.